2014 IEEE International Conference on Robotics & Automation (ICRA)
Hong Kong Convention and Exhibition Center
May 31 - June 7, 2014. Hong Kong, China

Aerodynamic Power Control for Multirotor Aerial Vehicles

Moses Bangura[1], Hyon Lim[2], H. Jin Kim[2] and Robert Mahony[1]

***Abstract*— In this paper, a new motor control input and controller for small-scale electrically powered multirotor aerial vehicles is proposed. The proposed scheme is based on controlling aerodynamic power as opposed to the rotor speed of each motor-rotor system. Electrical properties of the brushless direct current motor are used to both estimate and control the mechanical power of the motor system which is coupled with aerodynamic power using momentum theory analysis. In comparison to current state-of-the-art motor control for multirotor aerial vehicles, the proposed approach is robust to unmodelled aerodynamic effects such as wind disturbances and ground effects. Theory and experimental results are presented to illustrate the performance of the proposed motor control.**

I. INTRODUCTION

A multirotor aerial vehicle is a small-scale electrically powered aerial robot with four, six or eight rotors [1]. These vehicles have become the preferred platform for aerial robotics research due to their low cost, ease of design and simple dynamics [2].

There has been over a decade of work on modeling the flight dynamics of quadrotors [3], [1] and references therein. The common accepted model for rotor thrust and torque is a static relationship based on the square of the speed of the rotor [4] derived from analysis of hover conditions in still air. In recent years, this model has been found to be insufficient to account for the thrust generated from large displacements of air [5]. In [6], the authors applied momentum theory and blade element theory to incorporate translational velocities in the determination of thrust. Their approach in developing the model was based on sophisticated aerodynamic theory. The major drawback of their work is that they require aerodynamic parameters which are difficult to determine for low-cost blades that are mostly used on multirotor aerial vehicles. In performing a single stall turn, [7] developed detailed thrust models for different flight conditions based on momentum theory to account for these complicated aerodynamic effects. In 2012, [8], proposed a similar model that considers rotor speed, vehicle velocity, blade pitch and angle of attack, variables that are difficult to estimate during flight. A modified version that relates rotor speed to voltage was proposed in 2013 [9], although that model does not extend to incorporating translational and axial velocities.

Despite the potential limitations of the current state-of-the-art control of the propulsion system, quadrotors have been used in performing complex and aggressive manoeuvres.

[1]Australian National University, Canberra, ACT, Australia. {Moses.Bangura,Robert.Mahony}@anu.edu.au
[2]Seoul National University, Seoul, Republic of Korea {hyonlim, hjinkim}@snu.ac.kr

Fig. 1. **A quadrotor, the multirotor vehicle considered in this paper.** We propose a new motor controller that uses aerodynamic power as its desired output.

Some of these manoeuvres include the grasping and flights through narrow openings [10], multiple flips [11] and single stall turns [7]. To overcome limitations in the dynamic modeling of rotor thrust, these manoeuvers require sophisticated control techniques, both [10], [11] use iterative learning techniques to account for the unmodelled aerodynamic effects that come into play at high translational and rotational velocities, while [7] uses a more sophisticated aerodynamic model and introduces linear compensators that vary with the linear velocity of the vehicle to account for the unmodelled aerodynamics. High bandwidth control of actual thrust of a rotor based on local aerodynamic conditions of the rotor has the potential to overcome much of the complexity of these approaches. The authors showed in [12] that aerodynamic power can be used as the input or control variable for a multirotor system when the static rotor thrust model fail as a result of manoeuvres that are far from hovering condition. Although regulating aerodynamic power of a rotor is not the same as directly regulating the rotor thrust, the major advantage of this approach is that it is robust to changing aerodynamic effects such as translational lift, ground effect and axial displacement of the rotor. As such it is expected that the resulting thrust control will be more robust to external aerodynamic effects and perform better than current state-of-the-art control based on rotor RPM control and static hover thrust models.

In this paper, we present a novel motor control method for multirotor aerial vehicles based on regulation of aerodynamic power generated by the rotor. The approach depends on

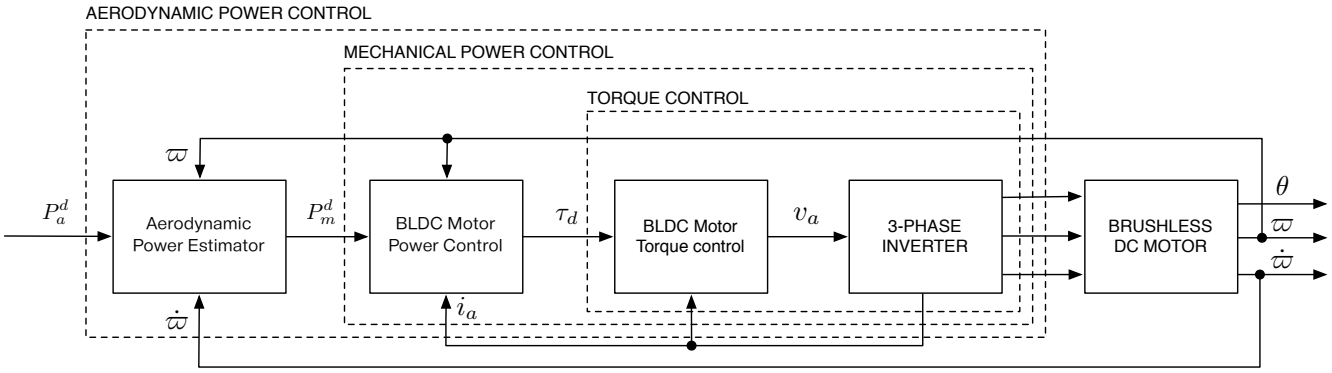

Fig. 2. **Proposed aerodynamic power controller architecture.** The proposed cascaded control architecture to effectively control the desired aerodynamic power.

programmable *electronic speed controllers* (ESCs) used for the *brushless direct current* (BLDC) motor for the quadrotor considered. By careful construction of suitable filtering algorithms, basic measurements of rotor speed and current for a given rotor can be used to generate estimates of electrical power consumed by the rotor in real time. The electrical power contributes to mechanical power injected into the rotor dynamics, aerodynamic power and some resistive loss in the motor. The figure of merit of rotor relates the mechanical power injected into a rotor to the aerodynamic power generated in hover conditions. Using a figure of merit estimate along with estimates of the resistive electrical losses of the motor ESC system, we propose a simple feedforward, proportional feedback control scheme to regulate aerodynamic power. To demonstrate the improved performance of the aerodynamic controller, we carry out a set of tests described in Section V-A. These tests explore the controller's ability in rejecting wind disturbances in axial and planar directions and validate the performance of the proposed approach.

The remainder of the paper is organised as follows: In Section II, we develop the theory behind the use of aerodynamic power in producing a desired thrust along with the motivation for changing the control input, in Section III, we show how the electrical properties of the motor can be used to estimate aerodynamic power, in Section IV, we present our aerodynamic power controller and in Section V, we present experimental results that illustrate the improved performance with the shift in control variable from rotor speed to aerodynamic power and the production of a desired thrust.

II. Aerodynamic Power as Output

In this section, we show why aerodynamic power should be the control variable for small-scale electrically powered multirotors. In addition, we also show how it can be obtained from the state of the vehicle.

A. Aerodynamics of flight

A multirotor vehicle achieves sustainable flight through aerodynamic forces generated from the four or more motor-rotor units. The aerodynamic forces generated by a motor-rotor unit are not only dependent on the physical dimensions such as radius, pitch, chord length of the rotors but also on the velocity of the column of air going through it. The velocity of the air column is also not only dependent on the rotor speed but also on wind velocity, objects and structures such as the ground and axial and translational velocities of the rotor plane [13].

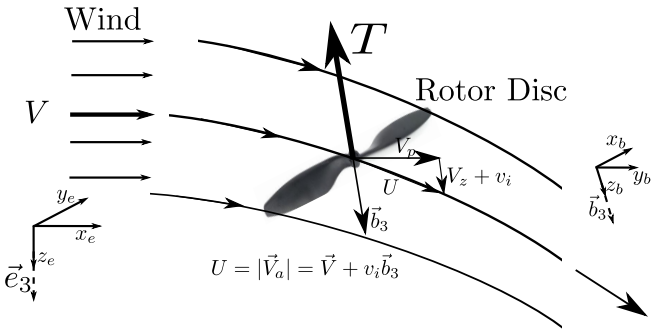

Fig. 3. **Momentum Theory control volume.** We represent the speed of the wind relative to the vehicle frame $\{B\}$, $V = |\vec{V}|$ and the total velocity of wind through rotor $U = |\vec{V}_a|$. As the wind goes through the rotor, its speed increases from $\vec{V}$ to $\vec{V}_a$ thereby creating thrust T from the power P_a in the air.

For rotor blades, the dynamic pressure and aerodynamic forces are created within one cycle of rotation as can be seen from blade element theory analysis [13]. Given that the rotors are usually rotating at speeds greater than 1000 *revolutions per minute* (RPM), one can assume that the aerodynamic forces have already been generated and have settled within the transient response times of the rotor speed and the estimated aerodynamic power. It will be shown in Section IV that the response time for both the aerodynamic power and rotor speed are under 100ms. This is far less than the attitude response time of quadrotors which is in the range of a few Hz [14]. Hence the transient response of the aerodynamic forces are negligible. Any unsteady aerodynamics causes magnitude and phase changes of the one rotor cycle aerodynamic forces. This is due to changes in the angle of attack of elements along the blade, induced velocity field and discrete tip vortices.

B. Thrust control

Let $\vec{v}$ be the velocity of the vehicle body frame $\{B\}$ to the inertial frame $\{A\}$ expressed in $\{A\}$, the rotation from body to inertia $R = {}^{A}R_{B} \in \mathrm{SO}(3)$, then the translational dynamic equation of state is given by (1) [14]

$$m\dot{\vec{v}} = mg\vec{e}_3 - F_T R\vec{e}_3 - R\vec{D}_T \in \{A\}, \tag{1}$$

where $\vec{e}_3$ is the unit vector along the z-axis in $\{A\}$, m is the mass of the vehicle, g is the acceleration due to gravity, $F_T = \sum_{i=1}^{N} T_i$ is the total of the thrust forces (T_i) produced by the N rotors and $\vec{D}_T$ is the sum of the rotor drag forces.

The current accepted models for thrust (T), torque (τ) and power (P) of the rotor are based on steady state analysis of hover conditions expressed explicitly as static functions of rotor speed. The standard expressions are

$$T = C_T\varpi^2, \tau = C_Q\varpi^2, P = C_P\varpi^3, \tag{2}$$

where C_T, C_Q and C_P are constants obtained from static tests. These models do not account for any of the aforementioned relative changes in the immediate airflow of the rotor. In particular, if the vehicle ascends or descends, translates, rotates, nears the ground or approaches obstacles, these aerodynamic relationships will fail.

To be able to account for the changes in thrust that result through changes in the state of the vehicle, we will use a momentum theory analysis. Consider the control volume shown in Fig. 3 where V is the free stream velocity, V_p is the magnitude of the velocity in the $x-y$ plane. It can also be seen that the velocity of the i^{th} rotor in the body fixed frame $\{B\}$ with magnitude V is $\vec{V}^i = [V_x^i,\ V_y^i,\ V_z^i]^\top$, where v_i^i is the induced velocity of the wind through the rotor. Using Momentum Theory, one can obtain the following equation for thrust [13]

$$T^i = 2\rho A v_i^i U^i, \tag{3}$$

where ρ is the density of the air column, A is the rotor disk area and the resultant velocity U^i of the air through the rotor is given by

$$U^i = \sqrt{{V_x^i}^2 + {V_y^i}^2 + (v_i^i - V_z^i)^2}. \tag{4}$$

Thus the thrust model is no longer expressed in terms of rotor speed but on the state of the airflow. Hence changes on the aerodynamic forces caused by relative velocity of the vehicle to the immediate air, obstacles and surfaces can now be accounted for. Also from momentum theory, the actual aerodynamic power in the airflow for the given thrust is given by

$$P_a^i = 2\rho A v_i^i U^i (v_i^i - V_z^i). \tag{5}$$

This shows that to produce a desired thrust given the state of the vehicle, aerodynamic power can be used as input to the propulsion unit. In doing so, the rotor speed increases or decreases depending on the conditions of the ambient airflow thereby ensuring that the aerodynamic power desired is that output into the airflow. This method of propulsion control is what we refer to as *aerodynamic power control*. Computing the desired rotor speed from (3) and (4) depends on blade element analysis and introduces considerable additional complexity [6].

C. Aerodynamic power control

Considering only the rotor and applying the conservation of energy, the following relation is obtained

$$P_m = P_a + P_{disp} + P_r, \tag{6}$$

where P_m is the mechanical power the motor shaft supplies to the rotor, P_a is the aerodynamic power supplied to the airflow, P_r is the power supplied in rotating the rotor, P_{disp} is the power dissipated by the rotors during the generation of the aerodynamic power. It is defined by

$$P_{disp} = P_a \frac{1 - FoM}{FoM}. \tag{7}$$

The *figure of merit*, FoM is a number between 0 and 1. It is the efficiency of the rotors in converting mechanical power to aerodynamic power at steady state [13]. Hence, one can rewrite (6) by

$$P_m = \frac{P_a}{FoM} + P_r. \tag{8}$$

If the torque through the rotor is τ, with the rotor rotating at a speed of ϖ and accelerating at $\dot{\varpi}$, then the mechanical power and power consumed by the rotor are obtained using the following relations

$$P_m = \tau\varpi, \tag{9}$$

$$P_r = I_r\varpi\dot{\varpi}, \tag{10}$$

for which I_r is the moment of inertia of the rotor. From these and an estimate of the FoM, the aerodynamic power can be estimated. Section III will show how one can explore the electrical state of the ESC-motor-rotor system in estimating P_a. In addition, it will be shown in the sequel how one can use aerodynamic power in the control of multirotor aerial vehicles.

III. MODELING OF PROPULSION SYSTEM

In this section, we describe the propulsion system of multirotors using a simplified model of a *brushless direct current* (BLDC) motor. With this model and the state of the motor-rotor system, we show how aerodynamic power is estimated.

A. Simplified brushless direct current motor model

In most multirotor systems, a BLDC motor is the main source for thrust generation. It is composed of a 3-phase permanent magnet synchronous machine and an electronic drive called *electronic speed controller (ESC)*. The name BLDC originates from the characteristics that its steady state response is similar to that of a brushed DC motor [15].

TABLE I

MOTOR-ROTOR PARAMETERS USED IN THIS PAPER

Parameter	Symbol	Value	Units
Back EMF constant	K_e	950	V/ϖ
Torque constant 1	K_{q_1}	0.0014	Nm/A^2
Torque constant 0	K_{q_0}	0.0242	Nm/A
Inductance	L_a	0.1	mH
Resistance	R_a	0.07	Ω
Rotor inertia	I_r	5.3847×10^{-5}	kgm^2
Viscous damping terms	b_1	2.9665×10^{-9}	-
	b_2	5.5613×10^{-6}	-

The steady-state electrical dynamics for a BLDC motor can thus be represented by the following set of equations [16]

$$v_a = K_e\varpi + i_a R_a + L_a \frac{di_a}{dt}, \tag{11}$$

$$\tau = (K_{q_0} - K_{q_1} i_a)\, i_a, \tag{12}$$

$$I_r\dot{\varpi} = \tau - D_r, \tag{13}$$

where D_r is the aerodynamic drag on the rotor, ϖ is the rotor speed, R_a and L_a are the resistance and inductance of the motor respectively. I_r is the rotor inertia and i_a and v_a are the current and voltage through the motor respectively. In most cases, BLDC motors for the propulsion system of multirotor vehicles are designed to have a very low inductance (e.g., $<$ 0.2mH) which implies that one can ignore the fast electrical dynamics within the 1kHz sampling frequency used in the implementation of the aerodynamic power controller. In order to account for the degrading rotor torque efficiency at high currents, we model the rotor torque constant by

$$K_q(i_a) = K_{q_0} - K_{q_1} i_a, \tag{14}$$

where K_{q_1} is an order of magnitude smaller than K_{q_0} which equals K_e but expressed in different units. The motor-rotor parameters used are summarised in Table III-A.

Instead of the normal linear relationship embedded in the viscous damping term or aerodynamic drag D_r, from static experiments, we model this by

$$D_r = b_1\varpi^2 + b_2\varpi, \tag{15}$$

where b_1 and b_2 are coefficients determined experimentally from noisy torque measurements. This is only used in the estimation of $\dot{\varpi}$, as such even in unsteady flows, one need not have a very accurate model for it because $\hat{\varpi}$ will go to ϖ ensuring that the correct $\dot{\hat{\varpi}}$ is obtained.

To estimate the aerodynamic power output of the motor-rotor system, accurate measurements of the rotor speed ϖ, rotor acceleration $\dot{\varpi}$, current consumed by the motor i_a and bus or battery voltage are required.

B. Measurement of internal variables

In the implementation of the proposed power controller, an ESC that is equipped with sensors for measuring the battery voltage, current and rotor speed was used [17]. For measuring ϖ, the ESC uses the rate of zero crossings within a fixed sampling window. The zero crossings of the free terminal among the three terminals determines the position of a magnet attached to the rotor for the next commutation. We used a 14-pole motor which provides 14 pulses per turn. For measuring currents, the ESC has a 0.5mΩ shunt resistor and an *analogue to digital* (ADC) converter for measuring bus or battery voltage.

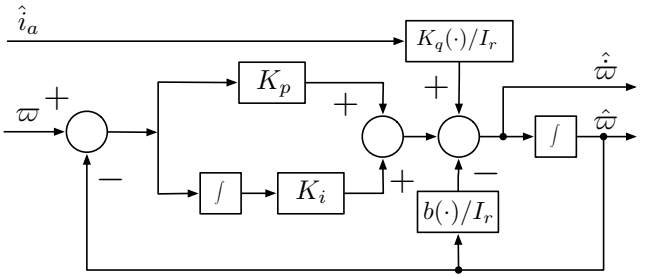

Fig. 4. **Rotor acceleration estimator.** The proposed complementary filter for the estimation of rotor angular acceleration ($\dot{\varpi}$).

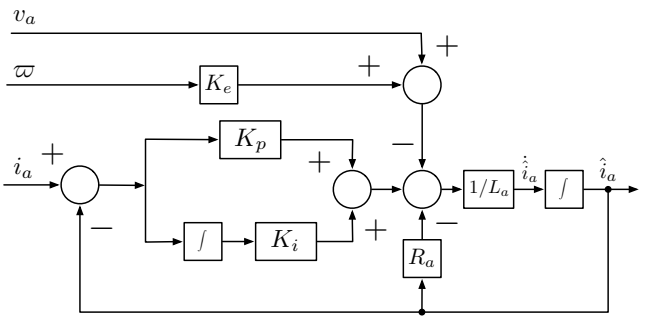

Fig. 5. **Current filter.** Schematic diagram of the proposed complementary filter for current.

C. Estimation of required variables for aerodynamic power

The noisy measurements of battery voltage, current i_a and rotor speed ϖ implies that some filtering and estimation of $\dot{\varpi}$ need to be carried out for the estimation and control of aerodynamic power. There are many possible filtering techniques that can be used. However, due to the limited computational resources and high bandwidth requirements preclude the use of techniques such as moving average filter or linear regression. This lead to the use of complementary filtering techniques.

Rotor acceleration $\dot{\hat{\varpi}}$ estimation. There is no direct measurement of the acceleration $\dot{\hat{\varpi}}$ of the rotor. Carrying out dirty time derivatives of rotor speed will give undesirable results due to the high frequency noise in rotor speed measurements. To this end, we propose the use of a complementary filter that combines (12) and (13). The Schematic diagram of the proposed $\dot{\varpi}$ estimator is shown in Fig. 4. The rotor drag D_r even if wrong, will be compensated for through the use of properly tuned innovation terms obtained from the first set of PI controllers [18]. The result of the estimation is shown in Fig. 6.

Current i_a filtering. We propose the use of the comple-

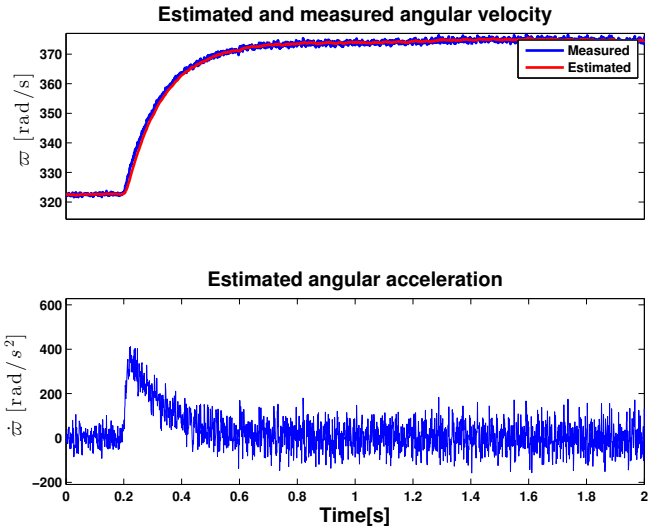

Fig. 6. **Rotor acceleration estimation result.** The ϖ and $\dot{\varpi}$ estimation results from the proposed complementary filter. The estimated ϖ result shows a lag of a few ms due to the nature of the filter. However, it is within an acceptable range of the sampling rate

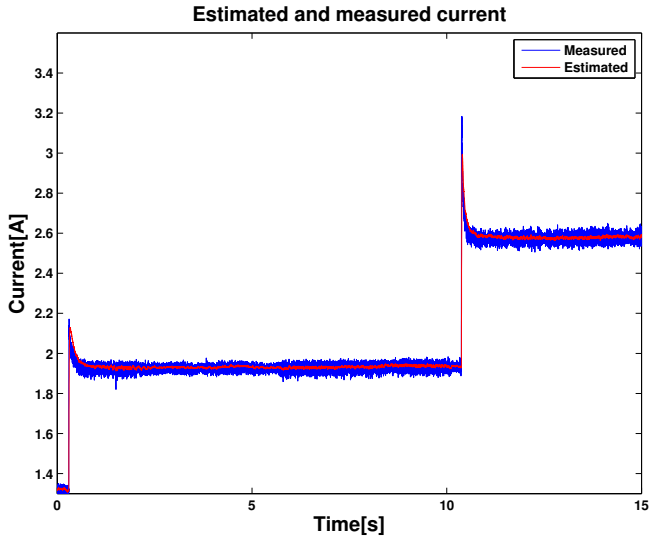

Fig. 7. **Current filtering result.** The filtered result has less noise than the measured current. The noise in the measurement is mostly due to high frequency switching noise within the miniature circuit board.

mentary filter shown in Fig. 5 to obtain estimates of i_a. It is implemented in the sense of (11). The estimation results of the current filter are presented in Fig. 7. It should be noted that despite not knowing an exact value for the inductance L_a, the innovation terms can be tuned to account for this.

D. Aerodynamic power estimation

Rearranging (8) and substituting for P_m and P_r with estimates of the electrical state obtained from measurements, the aerodynamic power is estimated using the following relation

$$\hat{P}_a = FoM(P_m - P_r) \tag{16}$$

$$= FoM\left((K_{q_0} - K_{q_1}\hat{i}_a)\hat{i}_a\varpi - I_r\varpi\hat{\dot{\varpi}}\right). \tag{17}$$

Hence the aerodynamic power output into the airflow is estimated from the measurements of the electrical state of the motor-rotor system.

IV. AERODYNAMIC POWER CONTROLLER

In this section, we describe our aerodynamic controller in detail (See Fig. 2). Unlike current rotor speed control, controlling aerodynamic power involves controlling both the rotor speed and current to reach the desired aerodynamic state. These two are competing variables linked by (11). Hence, we propose a cascaded control architecture for controlling aerodynamic power for small-scale electrically powered multirotor vehicles. The control architecture has current control in the inner-loop and aerodynamic power control in the outer-loop. The architecture is shown in Fig. 8. The controller determines the desired voltage v_a which is set as a fraction of the battery voltage. This fraction expressed as a percentage is known as duty cycle.

A. Current control

This is the inner-loop controller of our architecture. Its role is to enable faster transient responses in current and thus rotor speed. Looking at (12), it becomes obvious that controlling motor current is indirectly controlling rotor torque. Previous work on torque control of BLDC motors has been carried out in the electronics industry [19]. In the multirotor community, it has yet to gain any interest as the electric current is not the physical entity that interacts with the environment. With the 1kHz sampling rate, a system identification on current produces an unstable first order pole close to the origin. This unstable pole makes any high gain direct feedback control of current unstable. To avoid this and enable faster responses, we propose the use of a feedforward approach which ensures that higher electrical power is initially input into the system thus pushing the current and rotor speed to reach their desired states within a short period of time. The controller is shown in (18).

$$v_a = v_{ff} + K_{p_{i_a}}(i_a - i_a^d). \tag{18}$$

B. Aerodynamic power control

This forms the outer-loop of our cascaded controller. Its role is to regulate the aerodynamic power and ensure that it reaches the desired setpoint. To enable faster response without attenuating measurement noise, a feedforward voltage is determined based on the desired aerodynamic power.

From the schematic, the functions $f(P_a^d), f(v_a^d)$ are to be determined experimentally and are modeled by multiple order polynomial equations. $f(P_a^d)$ converts the desired power to desired voltage and $f(v_a^d)$ converts the desired voltage to desired current which is regulated in the inner-loop current controller. It should also be noted that one can use iterative Newton-Raphson methods to determine the desired feedforward states without using these polynomials. This is

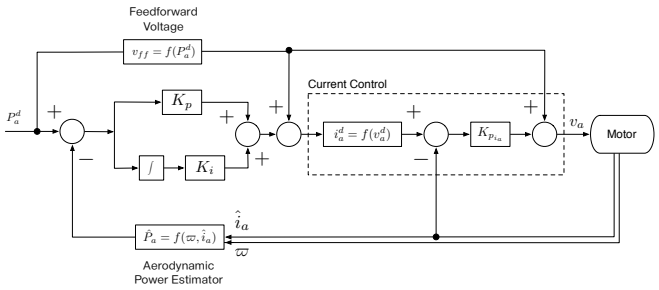

Fig. 8. **Aerodynamic power controller.** Schematic diagram of aerodynamic power controller with current control as the inner-loop.

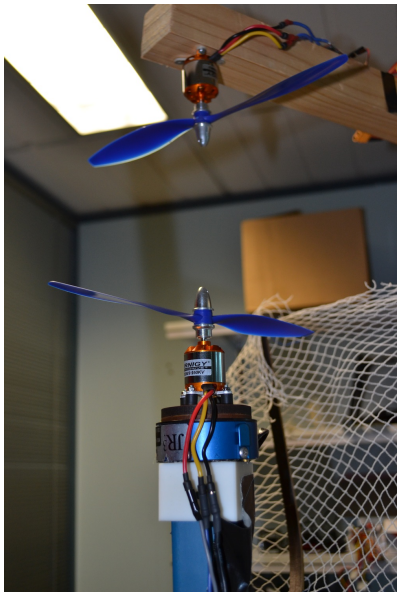

Fig. 9. **Experimental setup.** Consists of two rotors: disturbance generator and controller. This setup has a rotor generating wind to simulate axial movement of the rotor (and controller) attached to the force-torque sensor. For the different controllers, the same amount of wind is generated by setting a constant voltage in the disturbance generator to test responses.

possible through the use of the motor dynamic equations presented in (11) to (13) provided the motor parameters are well known.

V. Experimental Results

In this section, we present results that compare our proposed aerodynamic power controller to current rotor speed and open-loop voltage controllers. We carry out two set of experiments that are described in the sequel.

A. Static tests

The aim of the static test experiments is to compare the responses in thrust, rotor speed and aerodynamic power of the three controllers when subject to wind of $4\ ms^{-1}$ thereby simulating a $4\ ms^{-1}$ axial/translational velocity of the vehicle or $4\ ms^{-1}$ axial/translational gust at hover. One of the experimental setups is shown in Fig. 9.

The setup consists of an ESC which has the controllers and gives an output measurement of ϖ, i_a and $\hat{P}_a$ and a 6-axis force torque sensor [20] which outputs the thrust and

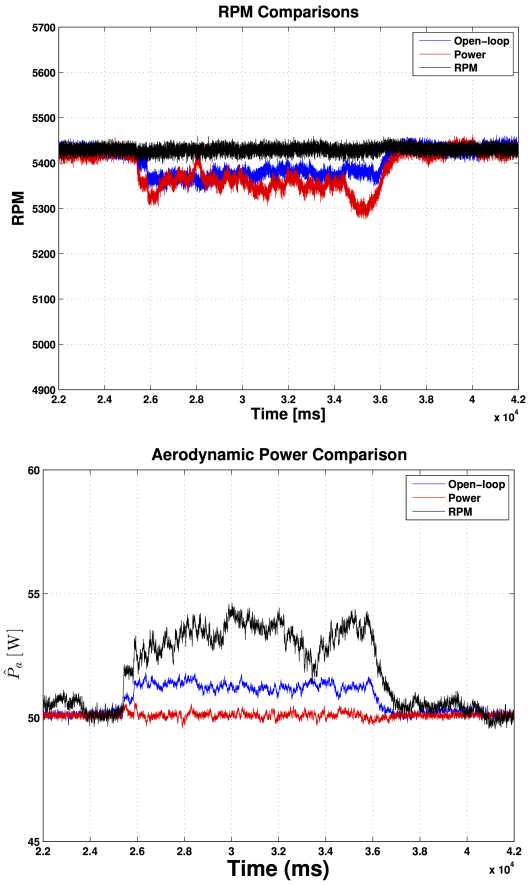

Fig. 10. **Experimental results (RPM and power) with $4\ ms^{-1}$ wind from sideways.** As is expected, power is supplied to the system which implies that the $\hat{P}_a$ of the rotor speed control goes up as it maintains a constant rotor speed. The power controller in trying to maintain a constant power in the airflow responds by causing a reduction in rotor speed.

torque measurements. In addition, there is a second rotor for the generation of the wind disturbance at a specified time during an experiment. We first perform two sets of experiments: 4m/s wind blowing axially down through the rotor and $4\ ms^{-1}$ sideways. The experiments were carried out for duty cycle ranging from 20 to 40% in increments of 2%. Figs. 10 and 11 show the response for side and axial wind respectively. Due to lack of space further results cannot be shown.

From the experiments, we can see changes in rotor speed, thrust and aerodynamic power. As is expected, the RPM controller maintains a constant rotor speed. The open-loop voltage controller, maintains a constant voltage whereas the aerodynamic power controller maintains a constant aerodynamic power. As such, in the case of the RPM controller, we see an increase or decrease in the aerodynamic power thereby reflecting whether power was added or removed from the system. The aerodynamic power controller in maintaining a constant desired aerodynamic power output causes changes in the rotor speed. When wind is blown from the top, the power controller increases the rotor speed in order to maintain a constant aerodynamic power thereby creating a

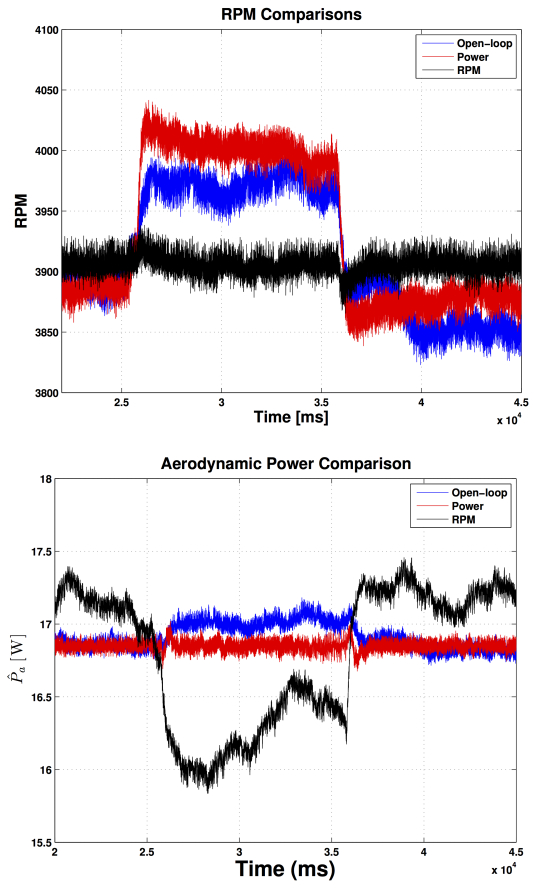

Fig. 11. **Experimental results (RPM and power) with** $4\ ms^{-1}$ **wind from axial direction.** By blowing wind from above unto the rotor indicates we are sucking power out of the airflow. In response to this, the aerodynamic power controller increases the rotor speed whereas the rotor speed controller maintains a constant rotor speed.

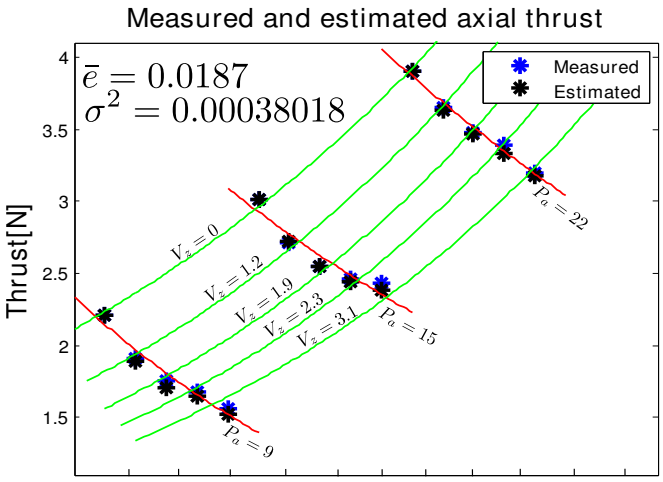

Fig. 12. Measured and estimated thrusts for axial tests showing that we can produce the desired thrust. This is indicated by the low mean and variance of the difference between the measured and estimated thrusts. Three sets of power experiments were conducted shown by the red lines. The green lines indicate the different axial velocities. The measured and estimated thrusts are indicated by star(*).

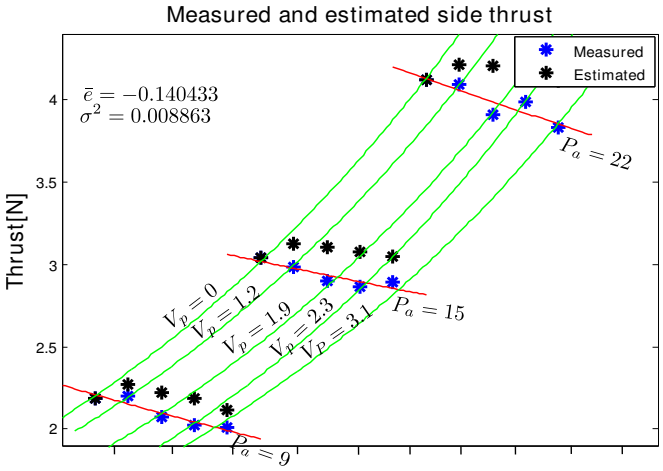

Fig. 13. Measured and estimated thrusts for planar tests showing that we can produce the desired thrust. This is indicated by the low mean and variance of the difference between the measured and estimated thrusts. Three sets of power experiments were conducted shown by the red lines. The green lines indicate the different planar velocities. The measured and estimated thrusts are indicated by star(*).

reduced impact on the total thrust produced. Unlike the rotor speed controller which sees a decrease in power of the system which causes a further reduction in thrust at a constant desired rotor speed. When wind is blown from the side, to maintain a constant aerodynamic power and thus thrust, the power controller decreases the rotor speed. However, the RPM controller in maintaining a constant speed, and reflecting the increase in power to the system, produces a further additional thrust. This additional thrust which has been observed in translational flights is referred to in the literature as *translational lift* [13]. This increase and decrease of rotor speed (hence much less effect on thrust) for the power controller implies that it is better at disturbance rejection compared to the current state-of-the-art rotor speed controller.

To show that with aerodynamic power as input, we can predict the thrust produced, we perform experiments that involve setting three different aerodynamic power with axial and translational velocities from 0 to 3 ms^{-1}. Using (4) and (5) and a few steps Newton-Raphson iteration, the induced velocity v_i is obtained. Thereafter the estimated thrust is determined using (3). Measured and estimated thrust for the three power settings and velocities are shown in Fig. 12 and Fig. 13 for axial and planar velocities respectively.

From the theory presented in Section II, changing the velocity implies that for a constant aerodynamic power, the induced velocity v_i of the airflow changes which causes a change in rotor speed and thrust. This is the change observed in the thrust produced by the aerodynamic power controller. The major advantage of the aerodynamic controller is that if we require constant thrust in the presence of translational and axial wind, the power can be changed accordingly to reflect this. Hence through power, we can set the exact desired power that can produce a given thrust that accounts for vehicle and airflow velocities.

VI. CONCLUSIONS

In this paper, we have presented a new controller for the propulsion system of small-scale electrically powered multi-rotors. We have demonstrated how the desired aerodynamic power input can be estimated using the electrical state of the BLDC motor. With this estimate, we have designed a controller that efficiently regulates aerodynamic power. We show that for a given desired thrust, and known translational velocity of a quadrotor, how the aerodynamic power that generates the desired thrust can be computed using momentum theory. In any case, using the proposed control to regulate aerodynamic power, the variation in thrust due to external aerodynamic disturbances is less than for current state-of-the-art motor control based on regulating rotor RPM. The new controller has been shown experimentally to resist changes in translational lift and thrust changes as a result of axial and horizontal airflow disturbances on the thrust generated.

ACKNOWLEDGEMENT

This work was supported by Australian Research Council through Discovery Grant DP120100316 and National Research Foundation of Korea (NRF) grant funded by the Ministry of Science, ICT & Future Planning (MSIP) (No. 2009-0083495, 2013-013911).

REFERENCES

[1] R. Mahony, V. Kumar, and P. Corke, "Multirotor aerial vehicles: Modeling, estimation, and control of quadrotor," *Robotics Automation Magazine, IEEE*, vol. 19, no. 3, pp. 20–32, 2012.

[2] H. Lim, J. Park, D. Lee, and H. J. Kim, "Build your own quadrotor: Open-source projects on unmanned aerial vehicles," *Robotics Automation Magazine, IEEE*, vol. 19, no. 3, pp. 33–45, 2012.

[3] P. Pounds, R. Mahony, and P. Corke, "Modelling and control of a large quadrotor robot," *Control Engineering Practice*, vol. 18, no. 7, pp. 691–699, February 2010. [Online]. Available: http://dx.doi.org/10.1016/j.conengprac.2010.02.008

[4] P. Bouabdallah, S. Murrieri and P. Sigwart, "Design and control of an indoor micro quadrotor," *Robotics and Automation (ICRA), IEEE International Conference on*, 2004.

[5] P. Martin and E. Salaun, "The true role of accelerometer feedback in quadrotor control," in *Robotics and Automation (ICRA), 2010 IEEE International Conference on*. IEEE, 2010, pp. 1623–1629.

[6] M. Orsag and S. Bogdan, "Hybrid control of quadrotor," *Control and Automation, IEEE Mediterranean Conference on*, 2009.

[7] H. Huang, G. M. Hoffmann, S. L. Waslander, and C. J. Tomlin, "Aerodynamics and control of autonomous quadrotor helicopters in aggressive maneuvering," in *Robotics and Automation, 2009. ICRA'09. IEEE International Conference on*. IEEE, 2009, pp. 3277–3282.

[8] C. Powers, D. Mellinger, A. Kushleyev, B. Kothmann, and V. Kumar, "Influence of aerodynamics and proximity effects in quadrotor flight," in *Proceedings of the International Symposium on Experimental Robotics*, June 2012.

[9] Y.-R. Tang and Y. Li, "Realization of the flight control for an indoor uav quadrotor," in *Information and Automation, 2013 IEEE International Conference on*. IEEE, August 2013.

[10] D. Mellinger, N. Michael, and V. Kumar, "Trajectory generation and control for precise aggressive maneuvers with quadrotors," *The International Journal of Robotics Research*, vol. 31, no. 5, pp. 664–674, 2012.

[11] S. Lupashin, A. Schollig, M. Sherback, and R. D'Andrea, "A simple learning strategy for high-speed quadrocopter multi-flips," in *Robotics and Automation (ICRA), 2010 IEEE International Conference on*. IEEE, 2010, pp. 1642–1648.

[12] M. Bangura and R. Mahony, "Nonlinear dynamic modeling for high performance control of a quadrotor," in *Australasian Conference on Robotics and Automation*, 2012.

[13] J. G. Leishman, *Principles of helicopter aerodynamics*. Cambridge University Press, 2006.

[14] H. B. M. Bouadi and T. M., "Modelling and stabilizing control laws design based on sliding mode for an uav type-quadrotor," *Engineering Letters*, 2007.

[15] P. C. Krause, O. Wasynczuk, S. D. Sudhoff, and S. Pekarek, *Analysis of electric machinery and drive systems*. Wiley. com, 2013, vol. 75.

[16] G. F. Franklin, J. D. Powell, and A. Emami-Naeini, "Feedback control of dynamics systems," *Pretince Hall Inc*, 1986.

[17] Autoquad Team, "The AutoQuad ESC32 - a yet unseen electronic speed controller," http://autoquad.org/esc32/, 2012, [Online; accessed 7-Aug-2013].

[18] R. Mahony, T. Hamel, and J.-M. Pflimlin, "Complementary filter design on the special orthogonal group so(3)," *Conference on Decision and Control*, 2005.

[19] Y. Liu, Z. Q. Zhu, and D. Howe, "Direct torque control of brushless dc drives with reduced torque ripple," in *IEEE Transactions on Industry Applications*, vol. 42, no. 2, 2005.

[20] JR3 Team, "JR3 Multi-Axis Load Cell Technologies," http://www.jr3.com/, 2013, [Online; accessed 31-Aug-2013].